RINGSTIFFNESS EVALUATION AND OPTIMIZATION OF STRUCTURED-WALL PE PIPES

F Fuerle[1], J Sienz[1], M Innocente[1], J.F.T. Pittman[1], V Samaras[2] and S Thomas[2]

[1] C[2]EC, School of Engineering, Swansea University, Wales – 398897@swansea.ac.uk; j.sienz@swansea.ac.uk
[2] Asset International Ltd., Newport, Wales

Structured-wall high density polyethylene pipes up to 3m diameter are used extensively in civil engineering applications including storm water attenuation tanks, culverts, surface drainage, inter-process pipe work, sewers etc. The pipes are manufactured by extruding a hollow box section which is wound in a spiral manner onto a mandrel with successive turns welded together using PE from an auxiliary extruder. A key quality control measure is the ring stiffness to BS EN 1446: 1996. The ability to predict this accurately as a function of the pipe wall geometry is a pre-requisite for optimization of the pipe design. The paper describes the development and the validation of finite element modeling of the ring stiffness test in comparison with experimental results, and considers the relationship between the test results and in-situ performance. Approaches to optimizing the pipe wall structure are also outlined.

Introduction

The structured wall pipes studied within the present work are produced by winding an extruded high density polyethylene (HDPE) box profile around a mandrel and welding each turn to the adjacent one (see **Fig. 1**).

Fig. 1 The extruded profile is wound around the mandrel and welded to the adjacent one.

The main objective of the current study is the development of a fast and accurate numerical simulation of the standardized ring flexibility test according to the standard BS EN 1446: 1996 (for more information the reader is referred to [1]). This standard specifies a method to measure the flexibility of a thermoplastic pipe with a circular cross section. To conduct such a test, an approximately 1-meter-wide pipe sample is placed in a compression testing machine, as shown in **Fig. 2**.

Fig. 2 A pipe sample placed in the pipe stiffness machine.

When compressing the sample between the two parallel plates, the machine monitors the force (F) that is necessary to move one of the plates with constant velocity. According to the standard, the ring flexibility (SN) is calculated at a vertical deflection equal to 3% of the pipe's inner diameter, as shown in **Eq. 1**

$$SN = \frac{F \cdot \left(0.0186 + 0.025 \cdot \frac{y}{D}\right)}{y \cdot L} \qquad \textbf{Eq. 1}$$

where *y* is the vertical deflection, *L* is the length of the pipe sample, and *D* is the inner diameter.

Future work will look at the improvement of the pipe's performance, as well as the minimization of the expended material. At the present stage the pipe's performance testing is restricted to that in the stiffness test. Thus the pre-requisite for the optimization of the pipe's profile is an accurate simulation of that stiffness test with low computational costs.

The present paper is structured as follows: First, the developed automated procedure for the generation of finite element (FE) models from scanned pipe profiles is discussed. Subsequently, several approaches to FE simulations are presented by looking at different element types and various possible boundary conditions. Those theoretical considerations are then amended by a convergence study. Furthermore a first application of optimization is outlined and finally the results of the work are presented.

Scan Processing and Automated Finite Element Model Generation

The theoretical, rectangular profiles of the pipes, extruded at the very beginning of the production process – completely defined by the height, width and wall thicknesses – significantly differ from the cross sections obtained after production, exhibiting differences of up to 20%. It should be noticed that the accurate measurement of the profile's height is of utmost importance, since it affects the moment of inertia with a power of three. Therefore, it was decided to cut samples of real profiles and scan their precise cross sections.

The scanning process returns files of discrete data points, distributed over the entire cross section. These points have to be processed prior to the creation of the finite element (FE) model. The programs carrying out that task are written in FORTRAN 77 and the whole procedure is controlled by means of a Java tool. The latter serves as a Graphical User Interface (GUI) and simplifies the use of the command-line-type FORTRAN programs. Furthermore it stores and manages the entered data. Java was chosen, since it provides a convenient way for the development of graphics, whereas FORTRAN impresses with its higher computational speed.

The scanning process starts with the rotation of the profile in a way that all walls are either horizontal or vertical. After that the repeating pattern can be identified, which is half of one box section. The identified repeating pattern and the rotated cross section are illustrated in **Fig. 3**.

The next step is the determination which points lie on the boundary of the cross section, since only those will be of use for the model generation.

The surface nodes are now divided into three lines: the "top", the "bottom", and the "C-shaped" lines. In **Fig. 4** they are referred to in as "line 1", "line 3", and "line 2", respectively.

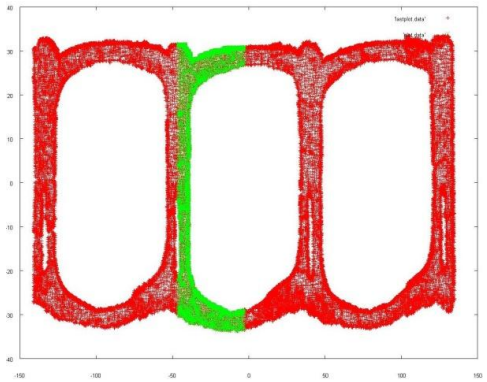

Fig. 3 Rotated profile with highlighted repeating pattern.

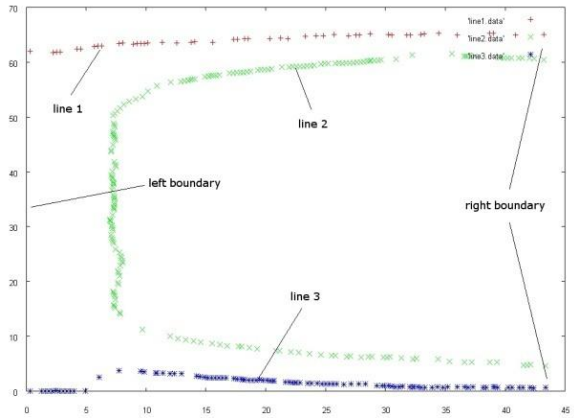

Fig. 4 Surface points separated into 3 bounding lines.

The three boundary lines have to be smoothed so that the resulting FE model does not exhibit unreal crooked edges that can cause singularities or stress concentrations. To this end, each of the three lines is replaced by a polynomial, whose parameters are found by the minimization of a least square function. That means the difference between existing discrete points and those from the polynomial is a minimum. The arising systems of equations during the determination of the coefficients of the polynomials are solved utilizing the open-source collection of mathematical subroutines LAPACK (see [2]) written in FORTRAN 77.

The generation of points that lie between the polynomial surface lines, and the definition of their corresponding thicknesses, are required for the generation of a FE model with shell elements. The procedure yielding these points starts by dividing the profile into an upper and a lower part. **Fig. 5** shows an example of the procedure for the upper part: First, a

straight line between points A and B is created. The midpoint M is obtained and a straight line perpendicular to segment AB, starting at M, is created. The intersections of this line with line 1, line 2 and the left boundary define the points O, P and Q, respectively. The shorter of the segments MO and MQ defines whether the controlling point is O or Q, and the point N is created as the middle point of the segment defined by the controlling point and P. This last segment defines the thickness corresponding to point N.
The procedure is repeated using points A and N as well as N and B, and so on, until the desired number of points is generated.

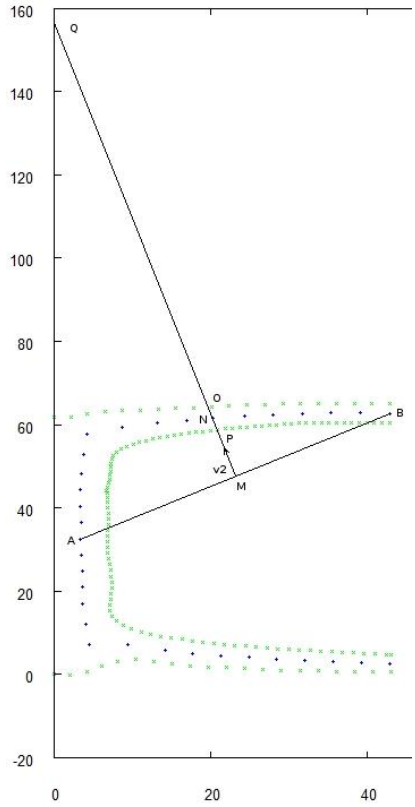

Fig. 5 Points' generation and thickness' determination for shell model.

An FE model can now be created with solid elements using the polynomial approximation, or with shell elements using the points on the profile's midsurface line with the corresponding thicknesses.
In a first stage of the present work, the commercial software package Altair Hyperworks (for further information see [3]) is used for the remaining pre-processing, processing and post-processing. The engaged tools from Hyperworks are Hypermesh (pre-processing), Optistruct (for further information see [4]) (FE solver) and Hyperview (post-processing). Hypermesh incurs the conversion of the point data into geometry data, as well as the discretization of the latter.
In order to speed up and automate the entire process, Hypermesh is accessed in batch mode instead of using the GUI. The communication is realized via command files which allow for the execution of all available tasks in the program.
The first command file written contains the geometry data and commands for the creation of the material, the element properties and for the mesh generation. Hypermesh is then called in batch mode, to process the command file, and to output a file containing the information of the mesh generated. Next, the user developed FORTRAN 77 program, which manages the procedure, reads this output file, applies the boundary conditions and writes another command file containing this information. Finally, Hypermesh is called again to process the latter and output the final model to be solved by Optistruct.
The above procedure is summarized in the flow chart in **Fig. 6**. It is characterized by two main features. The convenience of an automated procedure which allows for the simulation of the stiffness test of a certain pipe, is that nothing more than discrete data points of a scanned cross section and the diameter of the pipe have to be provided. At the same time the receipt of accurate geometry data is guaranteed. Summarizing one can say that a first step towards both accuracy and efficiency of the simulation has been made.

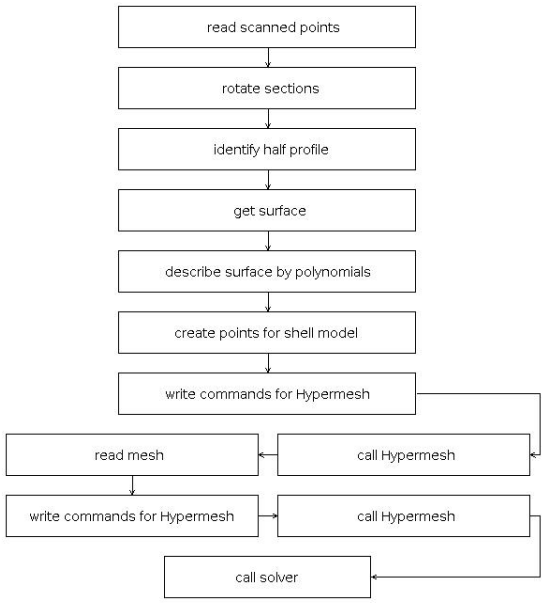

Fig. 6 Flowchart of the procedure for automated FE analyses.

In a later stage the entire Hyperworks package has been replaced by open-source software or self-developed programs. FEAP (for further information see [5]) was substituted for Optistruct, Paraview for Hyperview and a self-developed pre-processing tool for Hypermesh.

Finite Element Analyses

This section discusses the different degrees of accuracy and efficiency that can be achieved in the simulation of

the pipe stiffness test with the FE method. Numerous analyses are conducted in order to discuss and recommend a model with a suitable combination of accuracy and efficiency. For the simulations the material is modeled with a Young's Modulus of 1200 MPa and a Poisson ratio of 0.4.
The two main aspects to be considered are the type of element and the use of boundary conditions. The analysis code used within that investigation is Optistruct. In a later stage this solver will be partly replaced by the open-source solver FEAP. Simulations with either one will be of the linear static type. Therefore they cannot simulate the moving plate of the pipe stiffness experiment. The constant velocity plate movement is replaced by a prescribed displacement. Furthermore, this type of simulation assumes small strain theory which is acceptable considering a pipe displacement of 3% resulting in strains of at most 0.5%.

Element Types

Two main types of element can be considered to model this problem: "solid elements" and "shell elements". The former are 3D and describe the shape of the profile more accurately, while the latter are 2½D with a certain thickness assigned. Once decided upon the use of solid or shell elements, different shapes and either linear or quadratic interpolation are also available. Finally, an adequate mesh convergence study needs to be carried out.

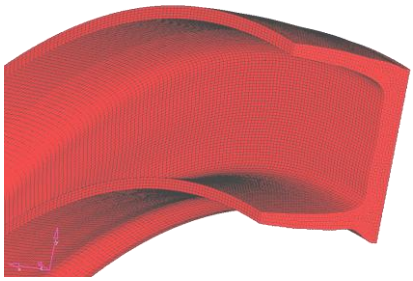

Fig. 7 Solid model illustration.

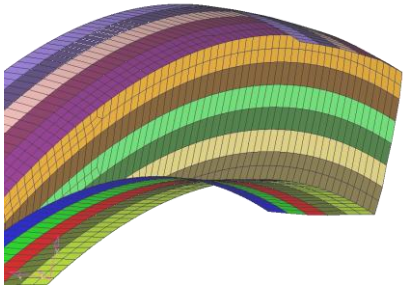

Fig. 8 Shell model illustration. Different thicknesses are defined along the cross section.

A solid element is commonly used for 3D structures with arbitrary shapes because the latter can be modeled with higher precision, at the cost of a higher computational effort (refer to **Fig. 7**).
Although there are numerous different types of solid elements available, only the linear (8 nodes) and quadratic (20 nodes) hexahedral elements and the linear (6 nodes) and quadratic (15 nodes) pentahedral elements were used in the current work.
A shell element is usually used for thin structures that present constant thicknesses. Since this is not the case for the pipe under study, the cross section is divided into smaller regions with constant thicknesses assigned. **Fig. 8** shows a shell model where different colors represent different thicknesses.

On the one hand, the use of shell elements results in models with lower numbers of degrees of freedom than the use of solid elements. On the other hand, however, this introduces further simplifications to the model that might affect the accuracy of the results. While the accuracy of the global behaviour might not be jeopardized by the use of shell elements, the local behaviour certainly cannot be simulated as detailed as this is possible with solid elements. This is because the geometry can not be represented as accurately.
The shell elements considered in the current work are the linear triangular (3 nodes) and linear quadrangular (4 nodes) elements. The corresponding quadratic elements have 6 and 8 nodes, respectively.

Boundary Conditions

The definition of the smallest model that can accurately represent the real problem directly affects the accuracy and efficiency of the simulation. In this regard, the exploitation of symmetries and definition of appropriate boundary conditions are as challenging as critical.
Clearly, both the geometry and the load state of the pipe subjected to the ring stiffness test are symmetrical with respect to all three coordinate planes. Therefore only one eighth of the whole pipe needs to be modeled, as shown in **Fig. 9**.

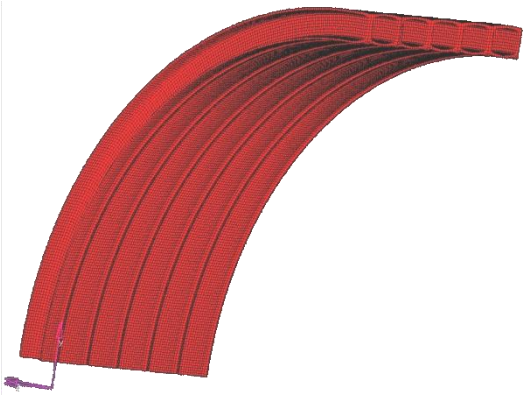

Fig. 9 Real repeating pattern (one eighth of the pipe).

The boundary conditions for this model are quite straightforward: free surface on the extreme of the pipe and no displacement on the faces cut by the symmetry

planes on the directions perpendicular to them or rotations about the axes contained in such planes. Finally, the displacements of the nodes in contact with the plate must be prescribed. However, in spite of the benefits of profiting from the symmetry planes, the model is still large and computationally expensive. The geometrically repeating pattern identified in **Fig. 3** makes it interesting to further reduce the model, although the geometrical symmetry is not extended to the boundary conditions. That is to say, the boundary conditions are not the same for every isolated geometrically repeating pattern. The latter, referred to as the "C profile" from here forth, is shown in **Fig. 7**.
If the C-profile is to be used to model the ring stiffness test, the question is what the appropriate boundary conditions are. A color-map of the displacements in the "x" direction for the model with the realistic symmetry exploitation (i.e. one eighth of the pipe) is shown in **Fig. 10**.

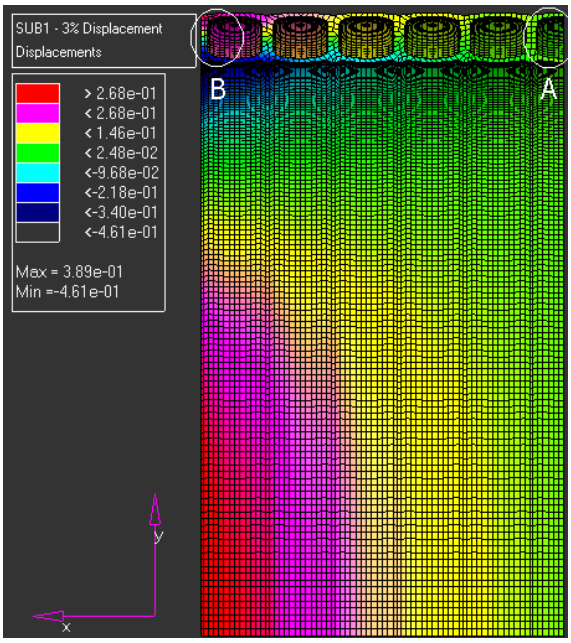

Fig. 10 Component "x" of the displacements for the real repeating pattern (one eighth of the pipe).

As it can be observed, the C-profile closest to the "yz" symmetry plane (marked "A" in **Fig. 10**) exhibits a behaviour that resembles the one it would have if the x-displacements of both its faces perpendicular to the "x" axis were restricted. On the contrary, the C-profile farthest from the "yz" symmetry plane (marked "B" in **Fig. 10**) effectively has one face unrestricted, and the overall behaviour resembles the one it would have if its opposite face was perfectly restricted, except for the additional distortion due to the accumulated displacements. The x-displacements scaled up, together with the corresponding color-map, are shown in **Fig. 11**. The additional distortion due to the accumulated displacements can be clearly seen for the right-most C-profile.
Therefore, there is no C-profile that can realistically model the behaviour of the pipe subjected to the ring stiffness test. The best that can be aimed for is to develop some artificial boundary conditions for a C-profile – without a real counterpart – that can "represent" rather than "simulate" the real problem. That is to say, this C-profile and its boundary conditions would not be simulating any of the C-profiles in **Fig. 10**. It must be kept in mind that these boundary conditions are unreal.

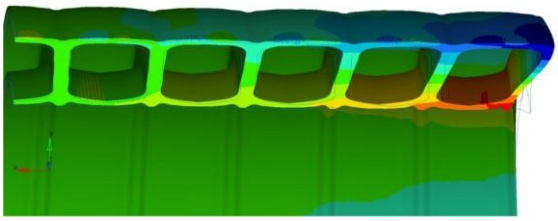

Fig. 11 Deformed shape of a quarter pipe with horizontal displacements scaled up.

It seems self-evident that the ring stiffness of the pipe in **Fig. 9** – with the real boundary conditions as described before – would be higher than that of the C-profile marked "A" in **Fig. 10** having the restrictive effect of the rest of the pipe simply removed (i.e. keeping its left "yz" face unrestrained). Similarly, the ring stiffness of the whole pipe would be lower than that of the same C-profile but now having the restrictive effect of the rest of the pipe replaced by a perfect restriction (i.e. forcing the x-displacements of its left "yz" face to zero). Hence the C-profile with the free border lower-bounds the ring stiffness of the pipe in **Fig. 9**, while the C-profile with the restricted border upper-bounds it. However, the range of ring stiffness values bounded by these two C-models might be quite wide. Therefore, some artificial intermediate boundary condition for the left "yz" face of the C-profile "A" needs to be conceived if a C-profile is to be used to model the ring test. The great advantage of this would be that the C-model is small enough to allow numerous analyses during the optimization to be carried out in a future stage. The model that simulates one eighth of the pipe could be used to verify the results returned by the C-model.
One way to realize this desired artificial boundary condition is to use spring elements as supports at the side, where the higher or lower restrictive effect desired can be controlled by tuning the springs' stiffnesses. Thus, the latter can be adjusted in such a way that the ring stiffness obtained by using the C-profile with springs matches that of the full pipe.
It is important to keep in mind that this model cannot be used to analyze the local behaviour of specific C-profiles, but to efficiently analyze the global behaviour such as the calculation of the ring stiffness.
The spring stiffness assigned to every single spring depends upon the size of the area that every spring stands for. Thus, the concept "lateral pipe stiffness" (*lps*) is introduced in **Eq. 2**, where S_{spring} is the spring stiffness, n_{spring} is the number of springs, A is the area that the springs are attached to, R_i and R_o are the inner

and outer radii of the pipe, and *h* is its height of the cross section.
This concept allows that, if changes in the geometry or discretization are made, the new spring stiffness can be determined from the constant *lps* without having to tune the former until the C-model results match those of the whole model.

$$lps = \frac{S_{spring} \cdot n_{spring}}{A} \qquad \textbf{Eq. 2}$$

$$A = h \cdot \frac{\pi}{2} \cdot \frac{(R_i + R_o)}{2} \qquad \textbf{Eq. 3}$$

Since the pipe should only be stiffened in the x-direction, the support of each spring on the extreme that is not attached to the pipe should only be restricted in that direction. This is a kinematic configuration (i.e. not entirely constrained), which cannot be handled by linear solvers such as Optistruct. This is overcome by restraining the support in all directions, but placing it far away from the pipe so that the components on directions other than "x" are comparatively negligible.

Convergence Study

Two different pipes were analyzed and compared to experimental data of real stiffness tests. The analyses included the model consisting of one eighth of the pipe and the C-models with different boundary conditions, as well as different element types and mesh refinements. Triangular and tetrahedral elements were avoided. The pipes have diameters of 1500 and 2100 mm. Most analyses were carried out for the "Pipe 1500". The "Pipe 2100" was merely used for the verification of the results.

Due to the axisymmetric geometry of the pipe, a 2D mesh is generated first, and then the 3D mesh is created by rotating the 2D mesh 90˚ about the axis of symmetry. The number of 3D elements that are created during the rotation of one 2D element will be called spin factor in following.
The convergence of the ring stiffness with respect to the mesh refinement was studied keeping a spin factor equal to 300, which means that 300 3D elements are created during the spin of a single 2D element. This results in the depth of the elements being equal to 4.1 mm (for the "Pipe 1500").
The convergence curves are shown in **Fig. 12**, where it can be observed that the convergence occurs for an element size of around 2 mm. Nevertheless, since the use of element sizes of around 3 mm to 4 mm results in slight variations of the ring stiffness, they are also acceptable.
Note that not only do these curves allow the study of the convergence but also the comparison between the different models. Thus, as anticipated before, the ring stiffness of the C-model with free boundary lower-bounds that of the whole model, while the ring stiffness of the C-model with restrained boundary upper-bounds it.

Of course it is to be expected that the most accurate simulation would be that of the whole model (i.e. one eighth of the pipe). Using this as a reference, the results obtained by the C-model with springs approximate the whole model with reasonable accuracy.
Aiming to define the depth of the elements, the analysis of the convergence of the ring stiffness with respect to the spin factor – and hence with respect to the elements' depth – was carried out for a 2D element size equal to 3 mm.

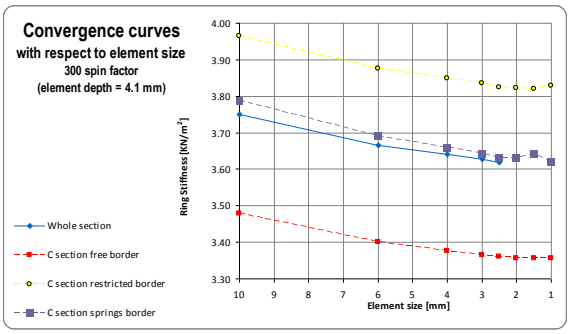

Fig. 12 Ring stiffness plotted against 2D element size for various solid models analyzed by Optistruct. The pipe's profile is 1500.

The resulting curves are shown in **Fig. 13**. Clearly, the ring stiffness is not very sensitive to the spin factor, and a value of 200 seems to be sufficiently refined. Therefore, it is concluded that an element size of 3 mm and spin factor of 200 (i.e. an element depth equal to 6.14 mm) lead to an appropriate refinement of the mesh for solid and linear elements, considering both accuracy and efficiency. The obtained simulated ring stiffness was approximately equal to 3.63 KN/m², while 3 lab experiments conducted by Asset returned an average ring stiffness equal to 3.71 KN/m² (exhibiting high standard deviation).

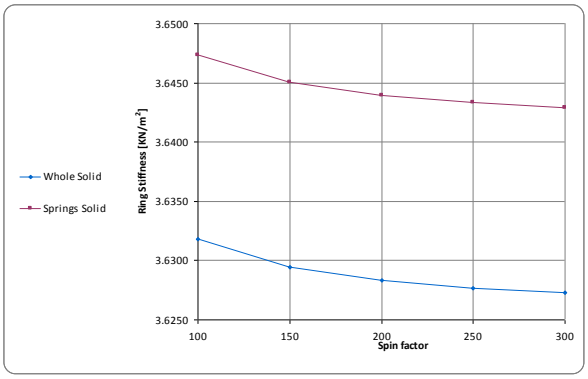

Fig. 13 Ring stiffness plotted against spin factor for different solid models analyzed by Optistruct. The pipe's profile is 1500.

Parallel to using solid elements, simulations using the more efficient shell elements were also implemented for the whole model, and for the three C-models: free, restricted, and with springs. The curves of the ring

stiffness convergence against the element size are shown in **Fig. 14**. It appears evident that the returned ring stiffness is not sensitive to the refinement of this mesh, although the degree, at which the local behaviour can be investigated, certainly is. That means a simulation with a coarser mesh might return the same ring stiffness as that of a finer mesh, but for instance the stress distribution can not be resolved as accurately. Hence, and given that the computational cost does not increase significantly for smaller sizes, an element size of 8 mm seems to be a good compromise.

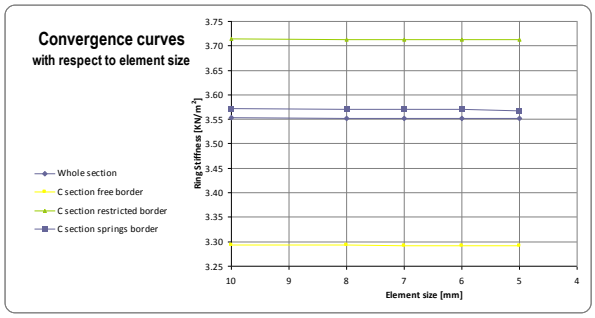

Fig. 14 Convergence of the ring stiffness with respect to the element size for different shell models analyzed by Optistruct. The pipe's profile is 1500.

It is important to remark that the time required for the analysis of a model discretized with shell elements is only a fraction of the solid counterpart. For instance, the whole model meshed with the recommended shell elements of 8 mm takes less than 15% of the running time of the same model meshed with solid elements of 3 mm and a spin factor of 200.

Optimization

In the optimization procedure, the shell models are created by utilizing B-splines (a detailed discussion can be found in [6]). They describe the centerline, as well as the varying thickness of the cross section. To this end *k* key points *P* are generated, as described before, whose *x* and *y* coordinates, as well as thickness values are known.
The profile is then divided into three segments – two horizontal ones and one vertical one. Now the variation of the three values (coordinates and thickness) along a segment is described by means of the B-splines, which are governed by the control values b_i. The corresponding *x* and *y* component form a control point B_i. Four control points build a sub segment, which is bounded by two key points.
A set of key points (black) and the corresponding control points (red) are depicted in **Fig. 15**.
With the control values computed, the splines can be evaluated at arbitrary locations, yielding the interpolated value for a coordinate component or the thickness.
The advantage of the above procedure, in comparison to using the key points straight away without interpolation becomes apparent, when applied in optimization processes. Here the control points are the design variables and not the key nodes. Therefore the geometry model is optimized, rather than the FE model. This leads to a smaller number of design variables while no accuracy is sacrificed. Furthermore, nodes will not be moved in a way that a different discretization stiffens the system, rather than an improved geometry.
Before the control values can be calculated the segments' end conditions have to be specified. There are two possible end conditions. The natural boundary condition, which features zero curvature at each end, is one.

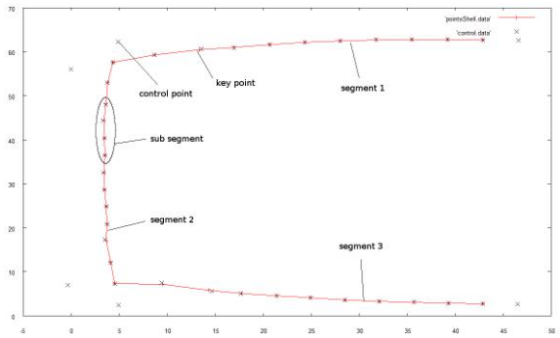

Fig. 15 Key points (black) and control points (red). Two key points and four control points build a sub segment. The cross section consists of three segments. Each segment is approximated by an individual B-spline.

The advantage of that condition is that no tangent vectors have to be provided. One should be aware though, that this can cause kinks at intersections of segments. These kinks lead to the so called C(0) connectivity. C(2) connectivity, offering smooth transition from one segment to another, can be achieved by choosing the second end condition. Therefore tangent vectors have to be chosen in such a way, that they match at each intersection.
Once the control values b_i are generated, a B-spline can be evaluated at an arbitrary position. This position is governed by the parameter *h*. This parameter starts with *0* at one key point and ends with *1* at the following.
With the B-spline definition completed, the optimization process can be constructed. The required elements are a program that can create the control points from discrete key points and thicknesses, as well as evaluate the B-splines to obtain discrete cross sectional points and its corresponding thickness. Additionally, an FE program has to be available. In the present case this is FEAP, extended by a user developed mesh generation tool. The last part is a software that improves the design variables in order to obtain an optimum configuration of those. The sensititivities of the objective function, in this case the cross sectional area, and of the constraint, that means

the pipe stiffness, required for this procedure have to be calculated as well.
The developed optimization procedure is illustrated in **Fig. 16** and can be described as follows: In a first step the control points of the B-splines are calculated and it is determined which are used as a design variables. In case of size optimization only those control values governing the thickness variation are used. In case of shape optimization also some of those describing the *x* and *y* coordinate variation are eligible.
Now the optimization tool, in this case a Sequential Quadratic Programming (SQP) tool (the theoretical background can be found in [6]), is initialized with the number of design variables and the number of constraints. Furthermore, the initial design variable values and their boundaries are defined. It returns the improved design variables.

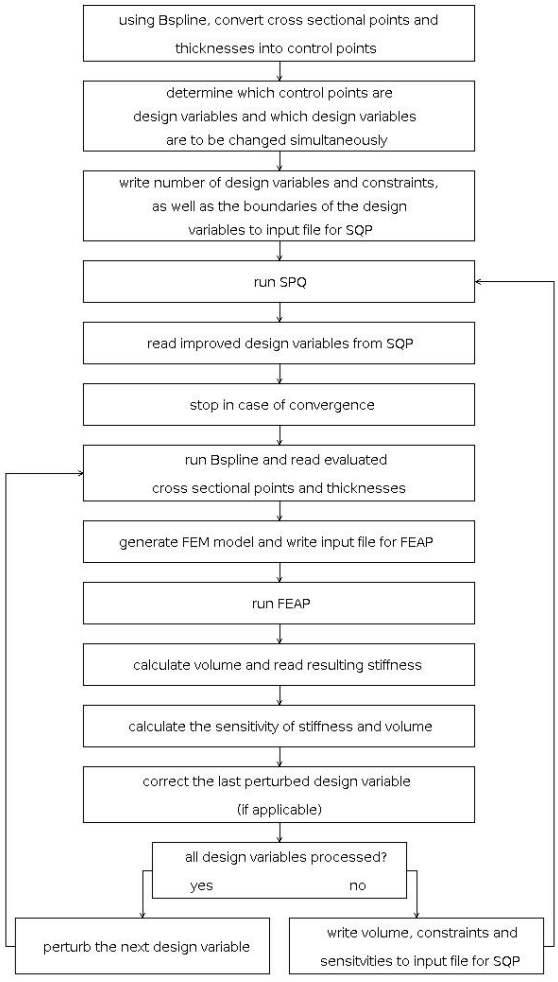

Fig. 16 Flowchart of the optimization process. Three programs, B-spline, FEAP and an SQP optimizer, are coupled and can be used for size and shape optimization.

Now the FEA part starts. One analysis is conducted without changing any of the design variables. All the following results within the actual iteration will be related to that initial analysis.
To run that initial analysis, the design variables from the SQP are read and via the B-spline tool the geometry is generated, which is converted into the FE model. After this is simulation is accomplished, the resulting pipe stiffness, as well as the cross sectional area are stored.
Subsequently n_{DV} analyses are conducted, where n_{DV} is the number of design variables. Those analyses distinguish by the design variable which is perturbed at the time. Comparing the resulting pipe stiffness and cross sectional area of the actual simulation with the initial one yields the corresponding sensitivity with respect to the active design variable. Naturally after an analysis with one perturbed design variable is finished, its pipe stiffness and area of the cross section are stored and its value is set back to the original one. This is repeated, until all design variables are processed.
The sensitivity of the objective function and the constraint with respect to the *i*-th design variable DV_i is computed according the finite difference method shown in **Eq. 4**.

$$\frac{df}{dDV_i} = \frac{f(DV_i) - f(DV_i + \xi \cdot DV_i)}{\xi DV_i} \qquad \textbf{Eq. 4}$$

Here $f(DV_i)$ is either the objective function or the constraint of the initial configuration, whereas $f(DV_i + \xi\ DV_i)$ is the one of a configuration where the *i*-th design variable is perturbed by a small factor ξ. This perturbation factor was found to be best as 10^{-4}.
Now the values of the objective function and the constraint as well as the corresponding sensitivities are written to a file that is read by the SQP. It then returns a set of improved design variables. The whole procedure is repeated, until convergence occurs.

So far the above procedure has been applied to the free C-shell model. The results have been compared to those obtained by Optistruct which has a built-in optimization tool. The design variables in either case were the thicknesses of the shell model. In the case of FEAP the control points governing the thickness distribution and in the case of Optistruct the actual shell element thicknesses.
The resulting optimum thickness variation can be seen in **Fig. 17**. It can be seen, that the commercial software Optistruct and the self developed tool, only consisting of open-source software, return very similar results. Note that the minimum thickness was set to 3mm.

Results and Discussion

The extensive convergence study of the FE mesh in the simulation of the stiffness test of the 1500 pipe leads to the following recommendations. The use of 2D element sizes of around **3 mm** to 4 mm and spin factors of around 200 (element depth of **6.14 mm**) are recommended for the **1500** diameter pipe. For other

pipes the spin factor can stay constant, whereas the 2D element size has to be adjusted in a way that the ratio between this and the element depth is around 2.05. Thus for the **2100** diameter one, this leads to a value of **4.2 mm** (element depth of **8.6 mm**).
For shell models, regardless of the pipe's diameter, an element size of **8 mm** is recommended.

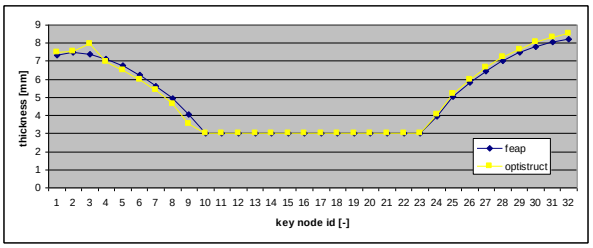

Fig. 17 Optimum thicknesses of the 33 key points, obtained by FEAP (blue) and Optistruct (yellow).

Depending on the purpose of a simulation, regarding the model type, different alternatives arise from this study. For instance, if accuracy is being sought and/or the analysis of local behaviour is of interest, the model should undoubtedly be the whole profile and the mesh should contain solid elements.
If efficiency is being quested instead, there are a number of options that offer different degrees of efficiency. The C-model with springs is fast and accurate but requires the tuning of the springs' stiffness and it does not represent local behaviour. The whole model with shell elements is not as efficient as any of the C-models but it is notably more efficient than the whole model with solid elements, while it can still represent local behaviour to some extent (e.g. stresses in the corners of each box-profile can not be analyzed accurately, but contrary to the C-models, the entire pipe is simulated, rather than an artificial substitute that merely yields the ring stiffness). Finally, the C-model with shell elements is the least accurate alternative, but the time required to obtain the ring stiffness makes it a candidate, if numerous analyses need to be carried out, for instance for optimization.

The results of the FE analyses using the whole and spring models, discretized with both, solid and shell elements, as well as available experiment data can be found in **Table 1** and **Table 2** for the 1500 and 2100 mm pipe, respectively.

	Test 1	**Test 2**	**Test 3**	**Mean**
experiment	3.74	3.79	3.60	3.71
	shell		**solid**	
	spring	*whole*	*spring*	*whole*
Optistruct	3.57	3.55	3.72	3.63
FEAP	3.61	3.62	n.a.	n.a

Table 1 Resulting pipe stiffnesses for the **1500** diameter pipe obtained from the solid whole model compared with an average pipe stiffness of real tests.

	Test 1	**Test 2**	**Test 3**	**Mean**
experiment	3.10	2.62	2.68	2.80
	shell		**solid**	
	spring	*whole*	*spring*	*whole*
Optistruct	2.58	2.59	2.68	2.58
FEAP	2.58	2.57	n.a.	n.a

Table 2 Resulting pipe stiffnesses for the **2100** diameter pipe obtained from the solid whole model compared with an average pipe stiffness of real tests.

The element sizes in all listed simulations are the recommended ones. It should be mentioned, that the reason, why the stiffness of the solid-spring model is higher than its shell counterpart, is that the spring stiffness was tuned, utilizing the shell model and due to the significantly coarser mesh in the shell model the tuning is subjected to a certain inaccuracy. Another tuning with the solid model would naturally eliminate this discrepancy.

The results of a first optimization are illustrated in **Fig. 18**.

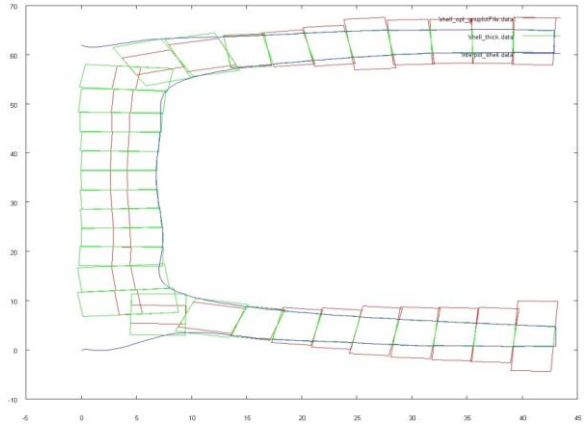

Fig. 18 Shell model. Thickness values of original (green) and optimized profile (red).

The objective was to minimize the area of the pipe's cross section (leading to less expended material) while its stiffness remains unchanged. The design variables were the control values of the B-spline that described the thickness variation. The original thickness values are shown in green, while the optimized values are in red. The blue lines show the true boundary of the model. Obviously, it is more efficient to concentrate the material in the middle of the two horizontal walls, while the material in the vertical wall does not contribute significantly. This improvement results in a reduction of the volume of 15.6%, from 1028.6 cm^3 to 867.8 cm^3.
The development of the objective function during the optimization process, i.e. the area of the cross section of the pipe is depicted in **Fig. 19**. The development of the constraint, i.e. the difference between the desired pipe stiffness and the computed one can be found in **Fig. 20**.

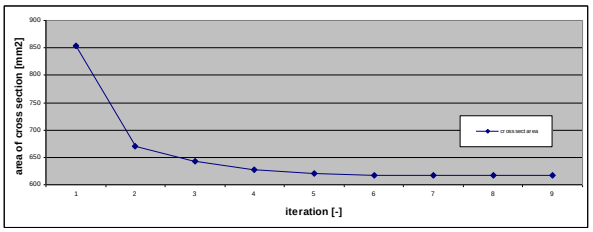

Fig. 19 Development of the objective function (area of cross section) with ongoing optimization process. An optimum solution minimizes the objective function.

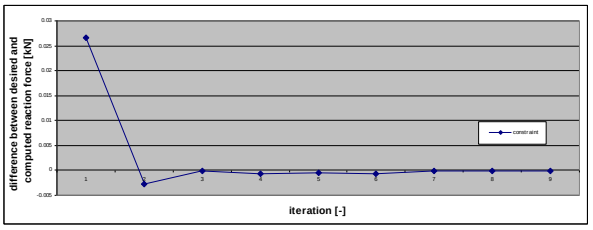

Fig. 20 Development of the constraint (difference between desired pipe stiffness and actual pipe stiffness) with ongoing optimization process. A solution is only accepted to be the optimum, if the constraint is smaller or equal to zero.

Conclusions

FE models with different degrees of accuracy and efficiency where sought for simulating the pipe stiffness test according to the standard BS EN 1446: 1996. This was realized, and a Java Tool and several FORTRAN 77 programs were developed, that allowed for an automated generation of those models from scanned pipe profiles, which guaranteed realistic geometry data.

Extensive convergence studies were carried out which allowed the recommendation of element sizes that satisfy a sufficient discretization and low computational costs.

Results from the FE analyses could be verified with real pipe stiffness tests. Given the deviation observed in those tests, the results can be called sufficiently accurate. The FE analyses were conducted with Optistruct and FEAP. Both solvers yielded almost identical solutions.

With those models at hand, an optimization tool, based on the coupling of open-source software, was developed. Its performance was successfully compared with the optimization tool built in the commercial software Optistruct.

Acknowledgements

The first authors gratefully acknowledge the financial support from Asset International Ltd.

References

1. British Standards Institution in *BS EN 1446 : 1996 –Plastics piping and ducting systems – Thermoplastics pipes – Determination of ring flexibility*; British Standards Institution, London, 1996.
2. Lapack, *LAPACK website*, http://www.netlib.org/lapack
3. Altair Hyperworks *Hypermesh Manual*, 2006
4. Altair Hyperworks *Optistruct Manual*, 2006
5. Berkeley University, *FEAPpv Manual*, http://www.ce.berkeley.edu/~rlt/feappv, 2005
6. E. Hinton; J. Sienz: M. Özakça in *Analysis and Optimization of Prismatic and Axisymmetric Shell Structure*; Springer-Verlag, London, 2003